A Wavelet Approach for the Detection of Rail Wheel Flats

S. Jia[1] and M. Dhanasekar[1]

Summary

This paper presents a wavelet approach to overcome the difficulties in the on-board monitoring and detection systems of rail wheel flats using vibration signals. Signal average techniques and wavelet local energy average concept are employed in this approach. A Matlab-Simulink based dynamic simulation system was also developed for the modelling of wheel flats and track irregularities. The analysis of the numerical simulation results demonstrated that the method proposed in this paper is effective for the on-board monitoring of wheel flats of sizes smaller than the condemning limits.

Introduction

Damage monitoring and detection of structures and components is critical to maintain safety and efficiency in the railway industry. This paper addresses wheel flats, a common form of damage that have the potential to generate serious impact forces sufficient to cause derailment due to failure of rails, axles, and/ or bearings. Currently wheels containing flats of 50mm are removed from service; the process of flat wheel condemnation being manual inspection. Automated techniques such as the way-side detection and on-board monitoring are increasingly becoming popular. As on-board techniques continuously monitor digital signals in real-time, they have the advantage of being integrated into the whole-of-train monitoring systems. Therefore we have addressed on-board system requirements in particular in this paper.

Although vibration signals are broadly used for damage monitoring in the industrial fields, such methods are not yet popular in railway engineering due to complications arising from track irregularities, train bogie system damping and loading variation that produce complex vibration signatures of the wagons. This paper presents a wavelet approach to overcome the difficulties caused by the complexities of wagon dynamics vibration signatures. Signal average techniques [1] and wavelet local energy average concept developed by Jia [2] are employed in this method. A Matlab-Simulink based dynamic simulation system was specifically developed for the modeling of wheel flats and track irregularities. The results demonstrate that the wavelet approach has the potential to be incorporated into the on-board monitoring systems.

A wavelet approach for the detection of rail wheel flats

The wavelet transform uses narrow time windows at high frequencies and wide time windows at low frequencies. Therefore, it has the potential to effectively detect transient

[1] Center for Railway Engineering, Central Queensland University, Rockhampton, QLD 4702, Australia

signals generated by local damages of components provided the interval and range of wavelet scale factor and the mapped wavelet coefficient three-dimensional diagram suitable for detecting the local fault are available. To overcome difficulties caused by such requirements, Jia [2] proposed a wavelet local energy average (WLEA) concept, based on the continuous wavelet transform for gear tooth damage detection. In this paper, a wavelet method for detecting rail wheel flat damage is obtained by combining WLEA concept with the synchronous signal average technique (that is analogous to denoising of complex signatures). Assuming $x(\theta)$ is the vehicle bogie average vibration signal in the wheel rotation angle domain and $\psi(\theta)$ is an analysing wavelet, the continuous wavelet transform (CWT) of $x(\theta)$ is given by,

$$W_x(a,b) = a^{-1/2} \int x(\theta)\psi^*(\frac{\theta - b}{a})d\theta \tag{1}$$

where a and b are the scale and angle parameter respectively.

If the average vibration signal $x(\theta)$ is transformed in scale range l_a (l_a also indicates the scale range width here), the WLEA in scale width l_a is defined as,

$$W_{LEA} = \frac{1}{l_a} \int | W_x(a,b) |^2 \, da \tag{2}$$

For $W_x(a_n, b_j)$, the wavelet local energy average is defined as,

$$W_{LEA}(b_j) = \frac{1}{N} \sum_{n=1}^{N} | W_x(a_{n,} b_j) |^2 \tag{3}$$

where a_n is the discrete scale factor, and b_j is the discrete angle location.

Based on equation (2) or (3), W_{LEA} versus b (or b_j) can be displayed in a two-dimensional diagram. In order to further emphasize the wheel flat impact contribution to the WELA, WELA variation along with wheel rotation angle θ is defined here as,

$$W'_{LEA}(b_j) = \frac{1}{N} \sum_{n=1}^{N} (| W_x(a_{n,} b_j) | - | \overline{W} |_n)^2 \tag{4}$$

where $| \overline{W} |_n = \frac{1}{J} \sum_{j=1}^{J} | W_x(a_{n,} b_j) |$.

Where wheel flats exist, W_{LEA} remains larger around the location of damage; this is emphasized by squaring of the coefficient of the wavelet transform in Eq. (2), (3) and (4).

Dynamic modelling of wheel flat vibration signature

There are many wagon dynamics simulation systems reported in the literature; here for simplicity, Lei's 2D model [3] is modified (Fig. 1) to account for wheels flats. A 2D 10 degrees of freedom (DOF) system was used to represent the wagon. Track system is modelled using a four DOF track element as illustrated in Figure 1(b). The sleeper mass and the partial ballast mass are lumped to the two ends of the beam element. The wagon and track system dynamics is expressed as,

$$[M]_{w/t}\{\ddot{u}\}_{w/t}+[C]_{w/t}\{\dot{u}\}_{w/t}+[K]_{w/t}\{u\}_{w/t}=\{F\}_{w/t} \tag{5}$$

where $[M]_{w/t}$, $[C]_{w/t}$, $[K]_{w/t}$, $\{u\}_{w/t}$ and $\{F\}_{w/t}$ are the mass matrix, damping matrix, stiffness matrix, displacement vector and force vector respectively; the subscript *w* stands for wagon and *t* stands for track.

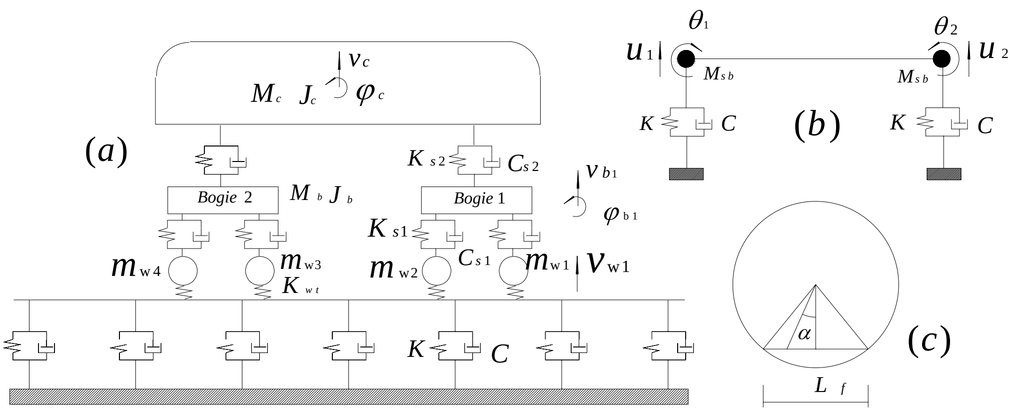

Figure 1. 2D model of wagon track system; Beam element & Wheel flat detail.

The Hertz interaction force between wheel and track is written as,

$$F_c=\begin{cases} G^{-3/2}|y_r|^{3/2}, & y_r<0\ , \\ 0, & y_r\geq 0\ , \end{cases} \tag{6}$$

where $G=4.57R^{-0.149}\times10^{-8}$ m/N $^{2/3}$ is the Hertz coefficient of contact between wheel and track; R is wheel radius. y_r is relative displacement between wheel and track. When including wheel displacement v_w, track displacement v_t, reduction of wheel radius due to flat damage $f_w = f(\alpha)$ (Figure 1(c)) and track irregularity v_{tir} into the relative displacement, y_r is calculated by,

$$y_r = (v_w + f_w) - (v_t + v_{tir}) \tag{7}$$

Typical measured data of track irregularity from an Australian rail track, illustrated in Figure 2, were used in the numerical simulation. All simulation cases were run by keeping the wagon speed constant at 30km/h.

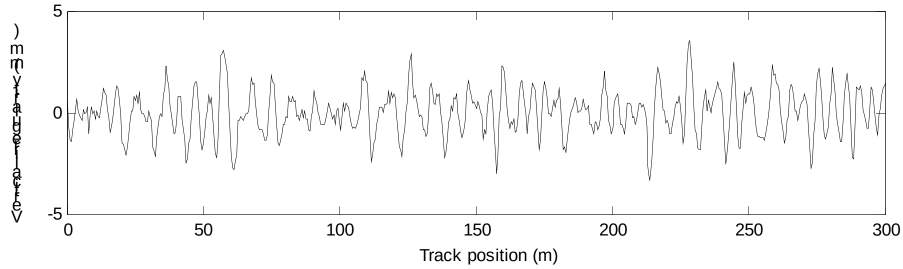

Figure 2. Track irregularity

In the numerical simulation, Eq. (5) was solved separately for the wagon and track. The interaction Eqs. (6) and (7) were used for coupling the two systems together. A MATLAB Simulink model, shown in Figure 3, was developed for this purpose.

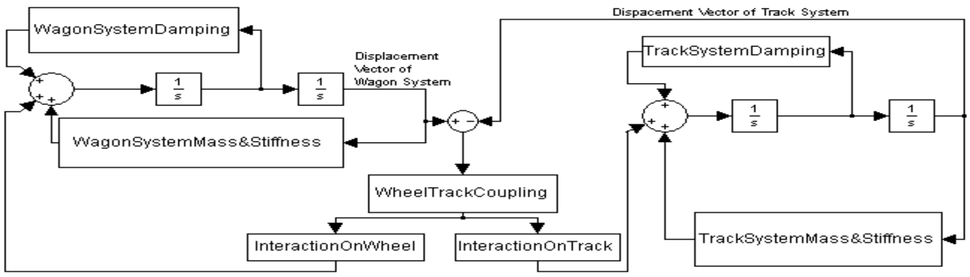

Figure 3. Simulink model of wagon and track coupling system

Result analysis and discussion

When using the wavelet transform to detect rail wheel flat damage, the wavelet function must be carefully chosen. The complex Morlet wavelet (Eq. (8)) was chosen for the analysis here because the shape of the transient vibration signal resulted from wheel flat damage is similar in nature to the Morlet wavelet.

$$\psi(\theta) = \sqrt{\pi \ f_b}\ e^{2\pi \mathrm{i}\ f_c\,\theta} e^{-\theta^{2}/f_b}\ , \tag{8}$$

where f_b and f_c are bandwidth parameter and wavelet center frequency respectively [4]. For the current analysis, f_b and f_c were set as $f_b = 1$, $f_c = 0.8$ and the range of scale a was set as [0.6, 76.8] with the interval Δa =0.6.

Figure 4 shows acceleration, 15 cycle acceleration average in wheel rotation angle domain and W'_{LEA} of the acceleration average of bogie. The first column (Fig. 4a, 4b & 4c) contains results for the analysis without wheel flat damage. The second column (Figs 4d, 4e & 4f) displays the results for 35mm wheel flat damage (L_f, Figure 1) and the third column (Figs. 4g, 4h & 4i) shows the results for 50mm wheel flat damage

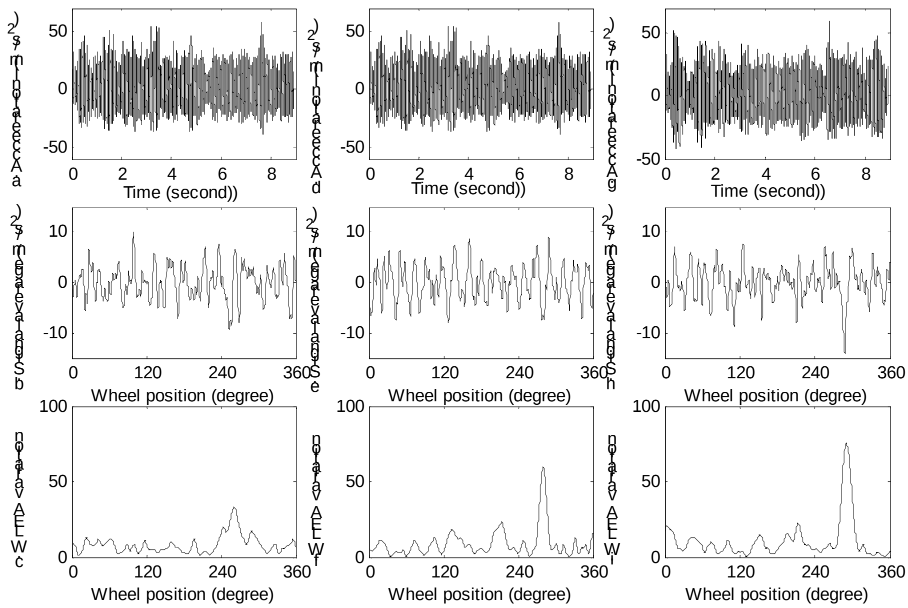

Figure 4. Bogie acceleration, acceleration average and W'_{LEA} of the average.

From the acceleration time series shown in Figs. 4a, 4d and 4g, the differences amongst the three cases of wheel flat damage could not be seen clearly. The signal averages displayed in Figure 4b, 4e and 4c, also do not distinctly differentiate the three cases. From the W'_{LEA} distributions of the three cases illustrated in Figs. 4c, 4f and 4i, the difference could be seen very clearly. In Fig. 4c, there is no obvious peak (no wheel flat). In Fig. 4f, there is a clear peak (35mm damage). In Fig. 4i, a larger peak is shown (50mm damage). These are reasonable results because the larger wheel flat produces the stronger impact leading to more energy to W'_{LEA} distribution. Figs. 5a, 5b and 5c are Polar drawing of W'_{LEA} distributions of the three wheel flat damage cases, which help with visually interpreting the effect of growing size of wheel defect damage easily.

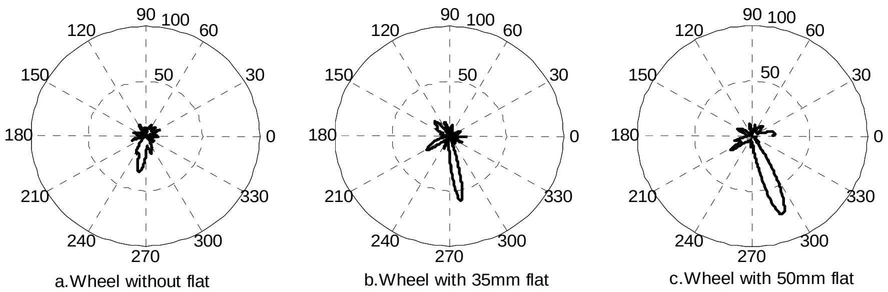

Figure 5. Polar drawing of W'_{LEA} distribution.

Conclusion

This paper presents a wavelet transform method combined with signal average technique for monitoring progressive growth in rail wheel flat damage from bogie acceleration signatures that result from both the track defects and wheel flats. Therefore this method could be regarded as a practical wavelet method for rail wheel flat damage on-board monitoring system. The approach proposed in this paper could be extended for monitoring and detection of damages in bearings and axles. Further research on vibration monitoring could greatly contribute to the integration of whole-of-train real time monitoring systems.

Reference

1 Stewart, R.M. (1977), "Some useful data analysis techniques for gearbox diagnostics", *University of Southampton Report MHM/R/10/77.*

2 Jia, S. (2004): *Dynamic Modelling and Diagnosis of Spur Gearbox Faults, PhD Thesis,* Curtin University of Technology, Australia.

3. Lei, X. and Noda, N. A. (2002): "Analysis of dynamic response of vehicle and track coupling system with random irregularity of track vertical profile", *Journal of Sound and Vibration,* Vol. 258(1), pp147-165.

4. The MathWorks, Inc. (2002): *MATLAB V 6.5 Wavelet Toolbox Manual.*